LIMNOLOGY
and
OCEANOGRAPHY: METHODS

Limnol. Oceanogr.: Methods 5, 2007, 328–337

Isotope disequilibrium and mass spectrometric studies of inorganic carbon acquisition by phytoplankton

Björn Rost[1], Sven A. Kranz[1], Klaus-Uwe Richter[1], and Philippe D. Tortell[2]*

[1]Alfred Wegener Institute for Polar and Marine Research, Am Handelshafen 12, 27570, Bremerhaven, Germany

[2]Department of Earth and Ocean Sciences, and Department of Botany, University of British Columbia, 6270 University Boulevard, Vancouver, British Columbia V6T 1Z4, Canada

Abstract

Given the need to assess potential effects of rising atmospheric CO_2 on aquatic primary productivity, many studies have investigated the physiological mechanisms of inorganic carbon acquisition by a variety of phytoplankton species. Membrane inlet mass spectrometry (MIMS) has become the preferred methodological approach for laboratory experiments, whereas the ^{14}C disequilibrium method has proven to be particularly useful for field studies. In the present investigation, we explicitly compare results of carbon acquisition measurements obtained with both of these approaches. Testing a range of phytoplankton species from different taxa, we show that both methods provide nearly identical results on the contribution of HCO_3^- and CO_2 relative to net carbon fixation. In contrast, although both approaches yielded highly reproducible estimates for extracellular carbonic anhydrase activity, the results differed significantly between the two methods. By directly comparing these two leading methods, we provide experimental confirmation of key assumptions used for data interpretation and discuss possible effects of assay conditions. Our analysis highlights the individual strengths and weaknesses of different approaches.

Over the past two decades, significant progress has been made toward understanding the physiological mechanisms of inorganic carbon (C_i) acquisition in marine and freshwater phytoplankton. This research recently has gained increased attention given the need to understand the potential effects of rising atmospheric CO_2 on marine primary production. While early studies suggested that phytoplankton could be growth-limited by the CO_2 supply in the ocean (e.g., Riebesell et al. 1993), subsequent laboratory and fieldwork has documented the existence of carbon concentrating mechanisms (CCM) in many phytoplankton species (Giordano et al. 2005 and references therein). The CCM – which functions to saturate C fixation by RubisCO – involves the active transport of CO_2 and/or HCO_3^-, as well as various isoforms of the enzyme carbonic anhydrase (CA) that catalyze the interconversion between these C_i species. The extent to which various taxa possess CCMs, and the relative efficiency of these C_i uptake mechanisms remain poorly understood. This information is needed to understand the effects of changing CO_2 levels on marine primary productivity and phytoplankton ecology (Giordano et al. 2005), and for the interpretation of ^{13}C signatures in marine organic matter (Laws et al. 2001 and references therein).

A variety of methods have been developed to examine C_i use by phytoplankton. Early work focused on kinetic approaches aimed at characterizing C_i affinities of cells and the O_2/CO_2 sensitivity of C_i fixation, providing evidence for the existence of C_4-like photosynthetic properties in phytoplankton (Graham and Whittingham 1968; Berry et al. 1976). Subsequent studies using silicone oil centrifugation methods (Badger et al. 1977, 1980; Kaplan et al. 1980) demonstrated that cells had the capacity to transport HCO_3^- and concentrate large intracellular C_i pools, whereas the activity of both intracellular and periplasmic carbonic anhydrase became apparent in a wide variety of phytoplankton taxa (Reed and Graham 1981; Aizawa and Miyachi 1986; Sültemeyer et al. 1993). More recently, the use of MIMS to study cellular CO_2 and O_2 fluxes has provided a new level of insight into C_i uptake by phytoplankton (Badger et al. 1994; Sültemeyer et al. 1995). In principle, MIMS can be used to measure intracellular C_i pool sizes,

*Alfred Wegener Institute for Polar and Marine Research, Am Handelshafen 12, 27515, Bremerhaven, Germany, Bjoern.Rost@awi.de

Acknowledgments

We thank Dieter Wolf-Gladrow, Lubos Polerecky, and two anonymous reviewers for constructive comments on the manuscript. This work is part of the multidisciplinary project BOOM (Biodiversity of Open Ocean Microcalcifiers), funded by the Institute Francais de la Biodiversité via the Agence National de la Recherche, grant ANR-05-BDIV-004. Funding for PDT was provided by the Natural Sciences and Engineering Council of Canada.

the kinetic properties of CO_2 and HCO_3^- transport, and the activities of intracellular and extracellular CA. This approach has proven extremely useful for integrated C_i uptake studies in phytoplankton, and, recently, has been successfully applied to a number of environmentally relevant marine species grown in laboratory cultures (Giordano et al. 2005). Although the MIMS is increasingly used in field studies (e.g., Tortell 2005; Tortell et al. 2006), the high cost and technical requirements for instrumentation remain a limitation. Moreover, MIMS analysis is not ideally suited for natural phytoplankton assemblages given the small net CO_2 and O_2 fluxes associated with many mixed autotrophic and heterotrophic communities.

Oceanographic field studies of C_i uptake by phytoplankton have thus far lagged behind laboratory work, and there have been relatively few published reports documenting the physiological mechanisms of C_i use by natural marine phytoplankton assemblages (Tortell et al. 2000; Tortell and Morel 2002; Cassar et al. 2004; Martin and Tortell 2006; Tortell et al. 2006). These studies have confirmed the existence of CCMs in situ, and demonstrated that HCO_3^- is a major source of inorganic C for photosynthesis in several ocean regions. For the most part, these field studies have relied on sensitive ^{14}C-based methods to estimate C_i uptake rates and the relative importance of extracellular CA activity. In particular, the isotope disequilibrium method (Espie and Coleman 1986; Elzenga et al. 2000) has proven to be useful for open ocean field work (Tortell and Morel 2002, Martin and Tortell 2006), and it is likely that this technique will be applied widely in future field studies of marine and freshwater phytoplankton assemblages.

As we progress in our understanding of C_i uptake by phytoplankton, it will become increasingly important to compare the results of laboratory and field experiments. This task is complicated by the different methods and protocols employed by various investigators. In most cases, independent methods are used to measure the same physiological parameters, yet the agreement between methods has not been explicitly examined. Moreover, each method has its own inherent assumptions that often are difficult to assess directly. A comparison of methods, therefore, is highly desirable. In this article, we present a comparison of two leading methods for C_i uptake measurements in phytoplankton. Using a range of phytoplankton taxa, we show that the isotope disequilibrium and MIMS methods provide very similar estimates of CO_2:HCO_3^- uptake ratios. In contrast, significant discrepancies exist in the estimates of extracellular CA activities. We discuss the individual strengths and weaknesses of the different approaches, and provide experimental confirmation of the key assumptions used for their interpretation.

Materials and procedures

Cultures conditions and sampling—For our method comparison, we chose to work with a variety of phytoplankton species (*Trichodesmium erythraeum* [IMS101], *Heterocapsa triquetra* [K-0481], *Emiliania huxleyi* [PML B92/11, highly calcifying strain], *Phaeodactylum tricornutum* [CCAP 1052/1A], *Thalassionema nitzschioides*, and *Phaeocystis globosa*) representing a wide range of taxonomic groups (cyanobacteria, dinoflagellate, coccolithophore, and diatoms) and functional modes of inorganic carbon acquisition. Cells were grown at 15°C in 0.2-μm-filtered seawater (salinity 34) enriched with nutrients according to f/2 medium (Guillard & Ryther 1962), except for *T. erythraeum*, which was grown at 25°C in artificial media YBCII (Chen et al. 1996). Acclimations were performed in dilute batch cultures (< 40 μg L^{-1} Chlorophyll *a*) under incident light intensities of 150 μmol photons m^{-2} s^{-1} and a light-dark cycle of 16:8 h, or 12:12 h in the case of *T. erythraeum*.

Cultures generally were sparged with air containing pCO_2 of 370 μatm (37.5 Pa) for all species except *P. tricornutum* which was cultured with 1800 μatm (182.4 Pa) CO_2 to minimize HCO_3^- use. Cultures of *H. triquetra* were not aerated as dinoflagellates are known to be negatively affected by the turbulence resulting from air bubbling (P.J. Hansen, pers. comm.). For this species, medium pH was adjusted to 8.0 and culture bottles closed with no headspace. Cultures in which the pH has shifted significantly from the target value (pH drift > 0.08) were excluded from further analysis. For all species, cells were acclimated to the respective carbonate chemistry for at least 5 d.

Prior to the measurements, cells were concentrated by gentle filtration onto polycarbonate membranes (pore size 3, 5, or 8 μm). During the filtration, culture media was exchanged with the respective assay buffer in a stepwise fashion maintaining the cells in suspension. Unless stated otherwise, cells were harvested simultaneously from the same culture flask and then were used in parallel assays (^{14}C versus MIMS). Both approaches yield estimates of the fraction of HCO_3^- versus CO_2 taken up by cells as well as the activity of extracellular carbonic anhydrase.

^{14}C disequilibrium measurements—The ^{14}C disequilibrium technique was developed to examine steady-state $^{14}CO_2$ and $H^{14}CO_3^-$ uptake by phytoplankton following a transient isotopic disequilibrium induced by the addition of a neutral pH $^{14}C_i$ spike into an alkaline pH cell suspension. The theory and methodology of this technique has been described extensively in several recent articles (Elzenga et al. 2000; Tortell and Morell 2002; Martin and Tortell 2006). Briefly, the method is based on the slow interconversion between HCO_3^- and CO_2, which allows differential labeling of these carbon species with ^{14}C over time periods of several minutes. In the C_i spike solution (pH 7.0) $^{14}CO_2$ represents 20% of the total DIC pool. In contrast, CO_2 accounts for only 0.4% of the total DIC in the cell suspension (pH 8.5) once equilibrium is reached. As a result, the specific activity (dpm mol^{-1}) of CO_2 in the $^{14}C_i$ spike solution is initially high, and it decays exponentially to an equilibrium value over the duration of the assay. If a phytoplankton species takes up CO_2 only, the ^{14}C incorporation rate should reflect these changes in the specific activity, i.e., high initial rates which decrease to lower values at equilibrium. The specific activity of $H^{14}CO_3^-/^{14}CO_3^{2-}$ (hereafter referred to as HCO_3^-) in the injected $^{14}C_i$ spike is close to its equilibrium

value and therefore remains nearly constant during the experiment. Consequently, species which use predominantly HCO_3^- as the carbon source show a near constant ^{14}C incorporation rate, i.e., a virtually linear time course of incorporation.

In practice, it is the accumulation of ^{14}C, rather than the instantaneous uptake rate which is measured in time-course experiments. As a result, the uptake curves are best modeled in their integral form (modified from Elzenga et al. 2000):

$$DPM_t = V_t(1\text{-}f)\,(\alpha_1 t + (\Delta SA_{CO2}/SA_{DIC})\,(1 - e^{-\alpha 1t}))/\alpha_1 + V_t(f)\,(\alpha_2 t + (\Delta SA_{HCO3}/SA_{DIC})\,(1 - e^{-\alpha 2t}))/\alpha_2 \quad (1)$$

V_t is the total rate of C_i uptake; f is the fraction of uptake attributable to HCO_3^-; α_1 and α_2 are the temperature-, salinity-, and pH-dependent first order rate constants for CO_2 and HCO_3^- hydration and dehydration, respectively (calculated as described by Espie and Colman 1986 with temperature and salinity corrections derived from Johnson 1982). Under the experimental conditions used for most experiments (15°C, salinity 34, pH 8.5) α_1 and α_2 are 0.0272 and 0.032 s^{-1}, respectively. For experiments conducted at 25°C, the constants were calculated as 0.0801 and 0.0977 s^{-1}, respectively. ΔSA_{CO2} and ΔSA_{HCO3} are the differences between the initial and equilibrium values of the specific activity of CO_2 and HCO_3^-; and SA_{DIC} is the specific activity of all inorganic carbon species at equilibrium. During steady-state photosynthesis, V_t and f are assumed to be constant so that changes in the instantaneous ^{14}C uptake rate reflect only changes in the specific activity of the two C_i species. The values of $\Delta SA_{CO2}/SA_{DIC}$ and $\Delta SA_{HCO3}/SA_{DIC}$ are set by the difference in pH between the ^{14}C spike and seawater buffer, with the values of 49 and –0.19, respectively.

In this study, we largely followed the experimental protocol described by Rost et al. (2006) with a few modifications. Concentrated cell suspensions were transferred into a cuvette (4 mL volume) with the respective media buffered at pH 8.5 (BICINE-NaOH, 20 mmol L^{-1}). After pre-incubation to 300 μmol photons m^{-2} s^{-1} for 6 min, a 10 μCi ^{14}C spike (37 MBq) of pH 7.0 (Amersham, CFA3, in HEPES, 50 mmol L^{-1}) was injected into the cell suspension. Afterwards, subsamples of 200 μL were withdrawn at short intervals and dispensed into 1.5ml of HCl (6 N) to stop C fixation. To remove residual $^{14}C_i$ (i.e., which was not fixed into acid-stable, photosynthetic products), samples were purged with air for at least 3 h. Following this, 10 mL scintillation cocktail (Packard, Ultima Gold AB) was added to the vials and the ^{14}C was measured by standard liquid scintillation procedures. To correct for any residual inorganic ^{14}C not removed by the degassing procedure, blanks consisting of spike added to cell-free buffer were measured and subtracted from all samples.

We ran the isotope disequilibrium experiments in two ways to examine CO_2:HCO_3^- uptake ratios and the importance of extracellular carbonic anhydrase activity. In the standard approach, potential eCA activity was eliminated by the presence of dextran-bound sulfonamide (DBS; Synthelec AB), a membrane-impermeable inhibitor of extracellular carbonic anhydrase. The inhibitor was added to a final concentration of 50 μmol L^{-1} at least 10 min prior to the experiments. In a modified approach (i.e., control experiments), incubations were also run without DBS in order to assess potential eCA activity in cells. For quantitative interpretation, the ^{14}C disequilibrium data were fit according to Eq. 1, using a Marqand-Levenberg non-linear regression algorithm. In the DBS run, the rate constants α_1 and α_2, were taken as the uncatalyzed values (see above), and the fraction of HCO_3^- take up by cells, f, was estimated (Elzenga et al. 2000) from the curve fitting procedure. In the control experiment, eCA activity was estimated from the data fits by allowing the rate constant, α_1, to vary as a model parameter whereas f was constrained to the value obtained in the DBS-treated sample (Martin and Tortell 2006). Values of α_2 can be calculated directly from α_1. Consequently, the modeled increase in the rate of HCO_3^-/CO_2 equilibration (hereafter referred to as α') was used to assess eCA expression. Extracellular CA activity (CA^{14C}) was expressed as:

$$CA^{14C} = (\alpha' - \alpha)/\alpha \quad (2)$$

MIMS: C_i flux measurements—The mass spectrometric technique uses the chemical disequilibrium between CO_2 and HCO_3^- during light-dependent C_i uptake to differentiate between CO_2 and HCO_3^- fluxes across the plasmalemma. Estimates of these fluxes were made using the equations of Badger et al. (1994). Briefly, C_i flux estimations are based on simultaneous measurements of O_2 and CO_2 during consecutive light and dark intervals. During dark intervals, known amounts of C_i are added prior to the initiation of the subsequent light interval. Rates of O_2 consumption in the dark and O_2 production in the light are used as direct estimates of respiration and net C fixation, respectively. Net CO_2 uptake is calculated from the steady-state rate of CO_2 depletion at the end of the light period, corrected for the CO_2/HCO_3^- interconversion in the medium. The HCO_3^- uptake is derived by a mass balance equation, i.e., the difference between net C fixation and net CO_2 uptake. As for all disequilibrium approaches, a lack of eCA activity is required, as this enzyme acts to rapidly dissipate CO_2/HCO_3^- disequilibrium in the cell boundary layer. The pseudo-first-order rate constant k_2 (formation of CO_2 from HCO_3^-) is determined experimentally from the initial slope of CO_2 evolution after injection of known amounts of HCO_3^- into CO_2-free buffered medium. The rate constant k_1 (formation of HCO_3^- from CO_2) is calculated from the product of k_2 and the ratio of CO_2 and HCO_3^- concentrations. Badger et al. (1994) provides more background on the numerical analysis of the data.

All MIMS measurements were carried out in an 8 mL thermostated cuvette, which was attached to a sectorfield multicollector mass spectrometer (Isoprime; GV Instruments) via a gas-permeable membrane (PTFE, 0.01 mm) inlet system. Prior to C_i flux measurements, the MIMS was calibrated for O_2 and CO_2 concentrations. Calibration for O_2 was achieved by measuring an air-equilibrated and oxygen-free assay buffer sample. The MIMS CO_2 signals were calibrated by injection of known amounts of $NaHCO_3^-$ into HCl (0.2 mmol L^{-1}). The CO_2 base-

line was determined by addition of 20 μL NaOH (10 mmol L^{-1}) into C_i-free media. Whereas the consumption of CO_2 by the MIMS is negligible, measured changes in O_2 signals were corrected for the O_2 consumption of the system. The simultaneously recorded background signal of argon, which is not affected by biological activities, was used to correct for small signal fluctuations in the oxygen signal. Assays were performed in the respective media, buffered with HEPES (50 mmol L^{-1}, pH 8.0). Light/dark intervals lasted 6 min and the incident photon flux density was 300 μmol photons m^{-2} s^{-1}. Concentration of DBS was 50 μmol L^{-1} to ensure the complete inhibition of any eCA activity.

MIMS: CA activity measurements—CA activity was determined from the ^{18}O depletion of doubly labeled aqueous $^{13}C^{18}O_2$ caused by several hydration and dehydration steps of CO_2 and HCO_3^- (Silverman 1982). This mass spectrometric procedure allows the determination of CA activity from intact cells under conditions similar to those during growth, and also can differentiate between intracellular and extracellular CA (eCA) activity (Palmqvist et al. 1994). Changes in the ion beam intensities corresponding to concentrations of the CO_2 isotopomers $^{13}C^{18}O^{18}O$ (m/z = 49), $^{13}C^{18}O^{16}O$ (m/z = 47) and $^{13}C^{16}O^{16}O$ (m/z = 45) were recorded continuously. The ^{18}O enrichment was calculated as:

$$^{18}O \log (\text{enrichment}) = \log((^{13}C^{18}O_2) \times 100)/\Sigma^{13}CO_2) = \log ((49 \times 100)/(45 + 47 + 49)) \quad (3)$$

CA assays were performed in f/2 medium, buffered with HEPES (50 mmol L^{-1}, pH 8.0) and were carried out in the dark. $NaH^{13}C^{18}O_3$ was added to a final concentration of 1 mmol L^{-1} and the uncatalyzed rate of ^{18}O loss was recorded for at least 8 min. Subsequently, 50-150 μL of cell suspension were added to yield a final Chl *a* concentration of 0.05-1.0 μg mL^{-1}. For the calculation of eCA activity (CA^{18O}), the linear rate of decrease in ^{18}O atom fraction after the addition of the cell suspension (S_2) was compared to the non-catalyzed decline (S_1) and normalized on Chl *a* basis:

$$CA^{18O} = (S_2 - S_1)/(S_1 \times \mu g \text{ Chl } a) \quad (4)$$

Assessment and discussion

The aim of this investigation was to compare different approaches for estimating CO_2 and HCO_3^- uptake and eCA activity in phytoplankton. We purposefully chose a diverse group of species with a wide range of carbon acquisition mechanisms and unique cellular architectures. As anticipated, we observed a large range in physiological characteristics among the species tested. For the purposes of this study, we shall not discuss these differences as they have been or will be addressed in other studies (Rost et al. 2003, 2006, Kranz et al. in prep.). Before comparing ^{14}C disequilibrium and MIMS results, it is important to summarize main assumptions underlying the calculations.

Assumptions of calculation—The interpretation of ^{14}C incorporation time-courses depends critically upon knowing the rate at which ^{14}C species approach equilibrium and the ratio of CO_2 to HCO_3^- in the ^{14}C spike and seawater buffer. In previous studies, these values have been derived from thermodynamic and kinetic constants published in the literature (Johnson 1982; Espie and Colman 1986). Here we used the MIMS to check the values experimentally for our buffer solutions.

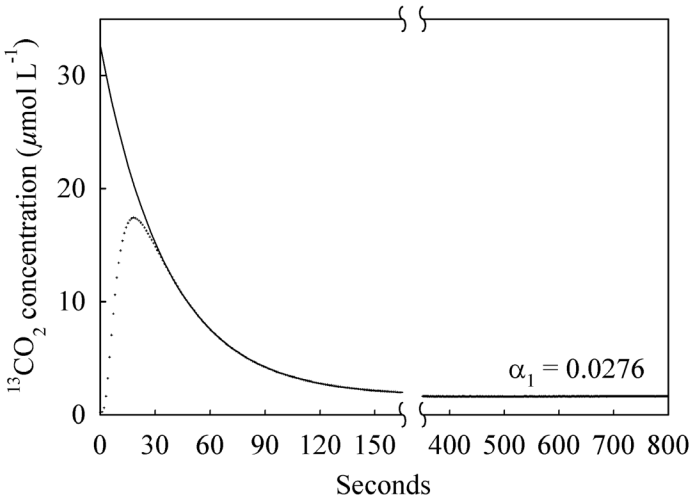

Fig. 1. Verification of theoretical rate constants from ^{14}C disequilibrium assay by MIMS measurements using ^{13}C as a tracer. At time zero, a $^{13}C_i$ spike (pH 7.0, HEPES, 50mM) was added into buffered media (pH 8.5, BICINE, 20mM) and the exponential decay of $^{13}CO_2$ into the HCO_3^- pool was monitored over time. Symbols represent measurements and the solid line represents a first order exponential decay fit to the data. The fit yielded a mean value for α_1 of 0.029 ± 0.004 s^{-1} (n = 6).

Central to the data analysis are the rate constants α_1 and α_2 that determine the time required for $^{14}CO_2$ / $H^{14}CO_3^-$ interconversion. In the absence of eCA activity, α_1 and α_2 are theoretically expected to be 0.0272 and 0.032 s^{-1}, respectively, under the experimental conditions used at 15°C. To verify these calculated values, the rate of C_i equilibration was measured under our assay conditions using ^{13}C as a tracer. For these tests, a $^{13}C_i$ spike solution (pH 7.0, HEPES, 50 mM) was added into buffered media (pH 8.5, BICINE, 20 mM) and the exponential decay of $^{13}CO_2$ into the HCO_3^- pool was monitored over time. In order to resolve the rate constants more precisely, the concentration of the C_i spike was twice as high as that used in the ^{14}C assay.

We found excellent agreement between theoretical and experimentally-derived rate constants. Figure 1 shows the time-course of $^{13}CO_2$ decay following the addition of the $^{13}C_i$ spike to the alkaline buffer at 15°C. The initial increase in signal intensity corresponds to the time required for homogeneous mixing and the response time of the sampling inlet and mass spectrometer. Beyond this initial rise, $^{13}CO_2$ concentrations subsequently decay exponentially as chemical equilibrium is approached. A first-order exponential decay fit to the data (ignoring the first ~ 30 seconds) yielded a rate constant (0.029 ± 0.004 s^{-1}; n = 6), which was practically identical to the theoretical calculations (0.0272 s^{-1}). It should be noted, how-

ever, that erroneous rate constants (resulting, for example, from small temperature shifts) cause a bias in f estimates. In species preferring CO_2 (f = 0.25), for instance, an overestimation in rate constants by about 10% would result in slightly higher estimates (f = 0.28) whereas estimates in HCO_3^- users (f = 0.75) are less sensitive to errors in the rate constants.

When the $^{13}CO_2$ decrease was extrapolated back to time zero, the predicted concentration added to the system was 33 μmol L^{-1}, a concentration that is very close to the theoretical value for a 20 μCi (74 MBq; SA ~ 55 mCi/mmol) spike into 4 mL assay media. Our calculations and experimental results (Fig. 1) indicate that $^{14}C_i$ additions greater than 10 μCi (37 MBq) under these conditions can introduce a significant perturbation in the carbonate system during the early part of the experiment, by elevating CO_2 levels. In contrast, the ^{14}C additions have only a minor (<5%) effect on total DIC concentrations in the seawater buffer.

In a second test, we used the MIMS to determine the relative proportions of CO_2 and HCO_3^- in our two experimental buffers (pH 7.0 and 8.5), as these ratios determine the initial and final conditions of the measurement. This was done by measuring the increase in CO_2 concentration upon additions of known amounts of C_i into the respective buffer. As with our determination of the rate constants, we also found excellent agreement between the expected and measured CO_2/DIC ratios. The measured values of 19.5% (± 1.5%; n = 4) in the pH 7.0 spike and 0.48% (± 0.11%; n = 6) in pH 8.5 media are not significantly different from those derived theoretically for use in our calculations (i.e., 19.5% and 0.4% CO_2 fraction, respectively). Thus, we are fully confident in the empirical constants used for our ^{14}C data analysis. Nevertheless, it should be noted that small changes in pH, both in the acidic spike and in the alkaline media, have large effects on the respective CO_2 fraction. The corresponding changes in ΔSA of the C_i species introduce an error in the f estimates derived from the model fit. In species preferring CO_2 (f = 0.25), for example, an overestimation of CO_2 fraction of the acidic spike by about 10% would cause the f estimate to be about 8% lower (f = 0.17) whereas f estimates in species preferring HCO_3^- are hardly affected.

The MIMS approach also relies on several key assumptions. The chemical disequilibrium between CO_2 and HCO_3^- during light-dependent C_i uptake is used to differentiate between CO_2 and HCO_3^- fluxes. O_2 fluxes are subsequently converted into carbon by applying a respiratory quotient (RQ) and photosynthetic quotient (PQ). Since the HCO_3^- uptake is derived from a mass balance between net CO_2 uptake and C_i fixation, the PQ directly affects the HCO_3^- uptake estimates. As in previous studies (e.g., Sültemeyer et al. 1995; Amoroso et al. 1998; Burkhardt et al. 2001), we applied values of 1.0 and 1.1 for the RQ and PQ, respectively. Underestimating the PQ would cause an overestimation of net C_i fixation and hence HCO_3^- contribution, whereas an overestimation in PQ would yield erroneously low HCO_3^- uptake.

The process of calcification (i.e., calcium carbonate production by cells like *E. huxleyi*) presents a further complicating factor for MIMS analysis. This process potentially affects the estimation of HCO_3^-/CO_2 uptake as an additional cellular C_i sink that is not accounted for in the calculations of Badger et al. (1994). However, since the HCO_3^- uptake is calculated from O_2-derived C_i uptake (i.e., photosynthetic C_i fixation) the influence of calcification on the calculations will only be small. The good agreement with HCO_3^-/CO_2 uptake estimates based on the ^{14}C method (see below), which is not affected by the photosynthetic quotient or the process of calcification, suggests that assumptions and calculations of the MIMS approach are robust.

Estimates for CO_2 and HCO_3^- uptake—Examples of ^{14}C incorporation time-courses by *P. tricornutum* and *T. nitzschioides* are given in Fig. 2. For *P. tricornutum*, identical time-courses were

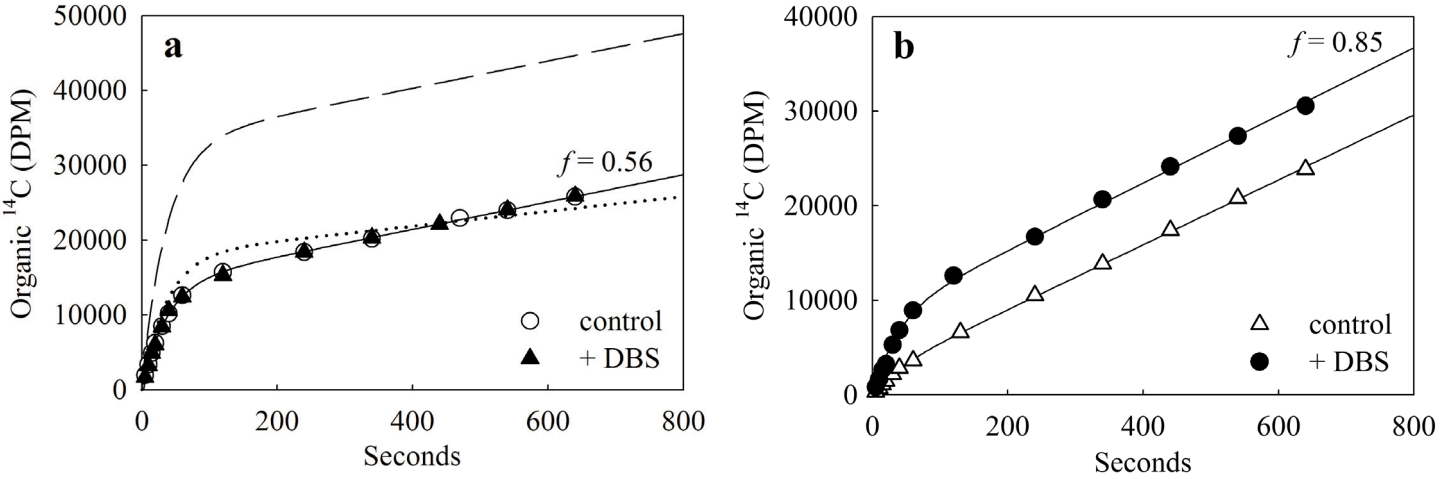

Fig. 2. Representative results from ^{14}C disequilibrium assays for *P. tricornutum* (a), and *T. nitzschioides* (b). Values of f shown on Fig. 2 represent the proportion of HCO_3^- uptake relative to net C fixation in DBS-treated cells (50 μmol L^{-1}), yielding values of 0.56, and 0.85 for the two species, respectively. The dashed lines represent best possible model fits with only CO_2 uptake, and the dotted curve in (a) represents the CO_2-only model fit constraining the final slope. Differences in ^{14}C incorporation between DBS and control, as seen in *T. nitzschioides*, were used to quantify eCA activities.

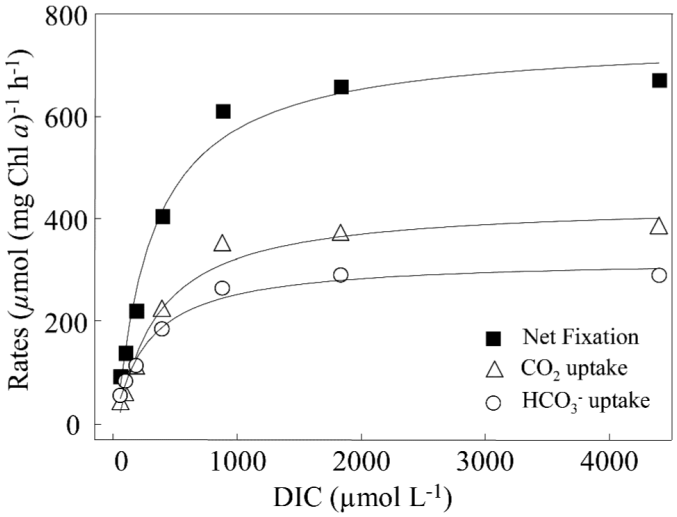

Fig. 3. Representative results from C_i flux assay showing Chl *a*-specific rates of net photosynthesis (squares), net CO_2 uptake (triangles), and HCO_3^- uptake (circles) as a function of DIC concentration in the assay medium for *P. tricornutum*. Curves were obtained from a Michaelis-Menten fit.

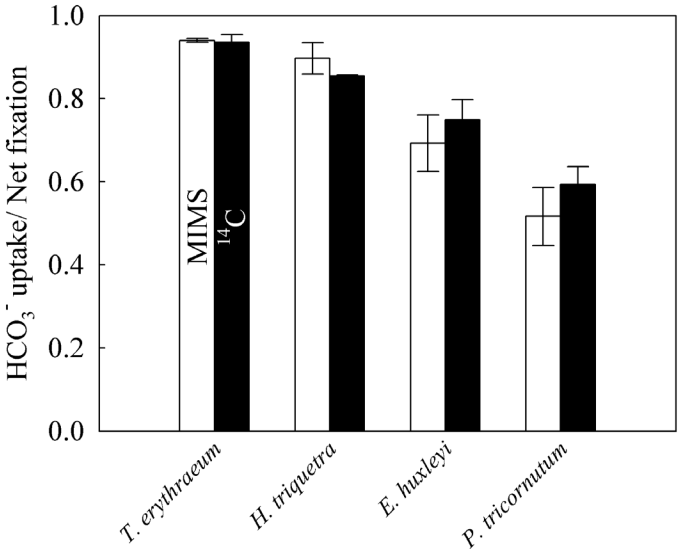

Fig. 4. Comparison of the HCO_3^- contribution relative to net C_i fixation obtained by C_i flux measurements (white columns) and ^{14}C disequilibrium technique (black columns) for the various phytoplankton species tested. Uptake ratios from MIMS measurements were based on the rates obtained at C_i concentrations of about 2 mmol L^{-1}. Values and standard deviations are based on at least triplicate measurements (n ≥ 3) and the same culture was sampled for simultaneous measurements using both techniques.

obtained in the presence and absence of DBS, indicating a lack of eCA activity in this strain as noted in previous studies (Burkhardt et al. 2001). The ^{14}C incorporation time-course obtained for this species could not be fit using a CO_2-only model (i.e., $f = 0$). As is evident from respective dashed and dotted curve (Fig. 2a), the observed C_i uptake curves cannot be fit without including a substantial contribution of HCO_3^- uptake. This is particularly obvious when final slope (V_t) is constrained to fit the observed slope (dashed curve on Fig. 2a). Values of f (the proportion of HCO_3^- uptake relative to net C-fixation) in DBS-treated cells were 0.56. For *T. nitzschioides*, there was a substantial difference between the time-course data for control and DBS experiments, indicating the presence of eCA activity (see below). As with *P. tricornutum* however, the time-course data could not be fit using a CO_2-only uptake model. Indeed, HCO_3^- accounted for the large majority of C uptake in *T. nitzschioides* with an f value of 0.85.

Representative results for C_i flux assays are shown for *P. tricornutum* (Fig. 3). Rates of net photosynthesis, CO_2 and HCO_3^- uptake were calculated and expressed as a function of DIC concentration. In order to compare these results with those obtained from the ^{14}C experiments we estimated the HCO_3^- contribution relative to net C_i fixation at DIC concentrations at ~2 mmol L^{-1}. For the data shown in Figure 3, the contribution of HCO_3^- was 0.45 under this external DIC concentration.

Comparison of the HCO_3^- contribution estimated from isotope disequilibrium results and MIMS analysis (at 2 mmol L^{-1} external DIC) revealed excellent agreement between the two methods for all species tested (Fig. 4). The methods produced similar results for "HCO_3^- users" such as *T. erythraeum*, "CO_2 users" like *P. tricornutum* as well as the calcifying coccolithophore *E. huxleyi*. The largest discrepancy between methods was observed for *P. tricornutum*. In this species, the ^{14}C disequilibrium technique yielded HCO_3^- contributions of up to 10% higher than those derived by C_i flux measurements. This difference was, however, not statistically significant (t test, $P > 0.05$), given the relative error associated with each measurement.

Estimates for CA activity—Whereas the MIMS has been used to measure CA activities for more than two decades, the modified approach of the ^{14}C disequilibrium technique recently was described by Elzenga et al. (2000). Examples of ^{14}C incorporation time-courses by *T. nitzschioides* are given in Fig. 2b. In contrast to *P. tricornutum*, ^{14}C incorporation differed significantly between control and DBS-treated cells, indicating the presence of eCA activity in this species. We used the isotope disequilibrium data to estimate the rate of CO_2/HCO_3^- interconversion in the cell boundary layer. To quantify this, the data from control (i.e., no DBS) experiments were fit while constraining f to the value obtained in the DBS-treated sample, but allowing α to vary (Elzenga et al. 2000, Martin and Tortell 2006). In the control for *T. nitzschioides*, α' was estimated to equal 0.19 s^{-1}, which is approximately a 6-fold enhancement of the non-catalyzed rate constant (α = 0.0272 s^{-1}).

Representative results from a mass spectrometric CA assay are shown for *T. nitzschioides* (Fig. 5). Changes in the ^{18}O-loss after the addition of cells compared to the spontaneous rate indicate significant eCA activity in this species. Activities for eCA by this approach are plotted together with those obtained

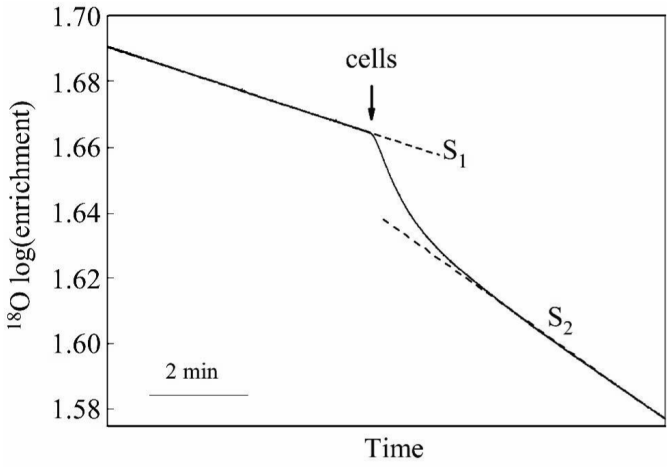

Fig. 5. Representative results for mass spectrometric CA assay with *T. nitzschioides*. Based on the concentrations of different CO_2 isotopomers $^{13}C^{18}O^{18}O$ (m/z 49), $^{13}C^{18}O^{16}O$ (m/z 47), and $^{13}C^{16}O^{16}O$ (m/z 45) the ^{18}O log(enrichment) is calculated. Activities of eCA are calculated by comparing the final linear rate of ^{18}O depletion (S_2) after the addition of cells with the initial linear slope (S_1), representing the uncatalyzed rate of ^{18}O exchange.

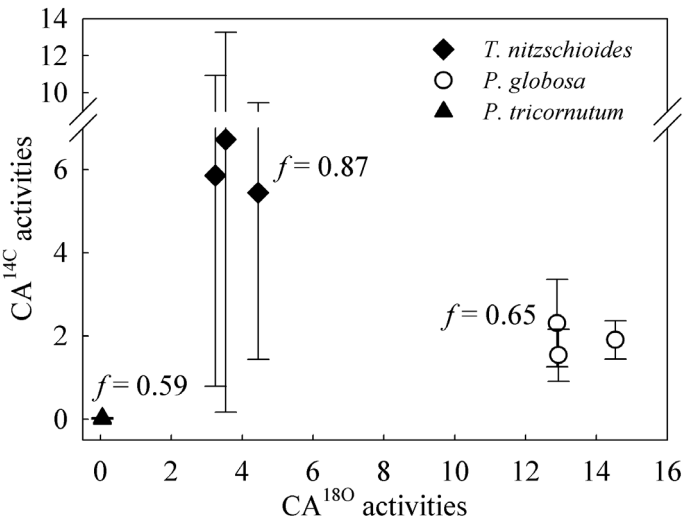

Fig. 6. Comparison of extracellular CA activities obtained by MIMS and ^{14}C disequilibrium technique with *T. nitzschioides*, *P. globosa*, and *P. tricornutum*. Values were estimated from control ^{14}C time course data, by fitting the data using Eq. 1, allowing α' to vary ($\alpha \geq 0.0272\ s^{-1}$), *f* was constrained to the value obtained in the DBS run. Activities obtained by MIMS were normalized to Chl *a* whereas activities obtained by ^{14}C were not normalized. Error bars represent standard error in α' estimates obtained by the model fit.

by ^{14}C technique in Figure 6, including also *P. globosa* and *P. tricornutum*. Both approaches yielded high eCA activities in *T. nitzschioides* and *P. globosa* and confirmed the lack of eCA in *P. tricornutum*. Unlike the estimation of *f*, however, the two methods yielded largely different values for activities, even when changes in α' were normalized to Chl *a* (data not shown). Moreover, errors in the ^{14}C derived CA estimates are much higher than those obtained by the MIMS approach. These findings can most likely be explained by inherent differences of the methods, which will be discussed below.

The ^{14}C disequilibrium technique assesses eCA activity by comparing the ^{14}C fixation modeled as an increase in α, hence by changes in the rate constants in the cell boundary layer. As a consequence, CA activity estimates reflect "effective activities" in the boundary layer and as such should be independent of the total biomass of plankton in the sample. In contrast, the MIMS approach quantifies bulk eCA activity in suspension by monitoring the changes in ^{18}O loss of doubly labeled HCO_3^-. These "quantitative activities" are clearly biomass-dependent and have to be normalized. In other words, whereas the MIMS measures eCA activities directly by its effect on the interconversion of CO_2 and HCO_3^-, the ^{14}C technique derives eCA activities indirectly by comparing the ^{14}C uptake kinetics in the absence and presence of DBS. Based on these considerations, one could expect that ^{14}C-based "boundary layer" estimates are higher than those ^{18}O-based "bulk" estimates of eCA activities. This is only true, however, for *T. nitzschioides* and not *P. globosa*. A further reason for the discrepancy may be the fact that eCA activities are measured in the dark for MIMS and in the light for the ^{14}C method. Potential light-activation of eCA, as has been suggested by Nimer et al. (1998), is consequently not accounted for by the MIMS approach.

Estimates for eCA activities by the ^{14}C approach showed high errors for *T. nitzschioides* whereas in *P. globosa* and *P. tricornutum* the errors in α were much smaller (Figure 6). To understand this result, we applied the model (Eq. 1) to a series of hypothetical ^{14}C time-course experiments with different *f* and α values (Martin and Tortell 2006). A random error of up to 5% was introduced to simulate experimental noise in the test data sets. The results given in Fig. 7 indicate that the curve-

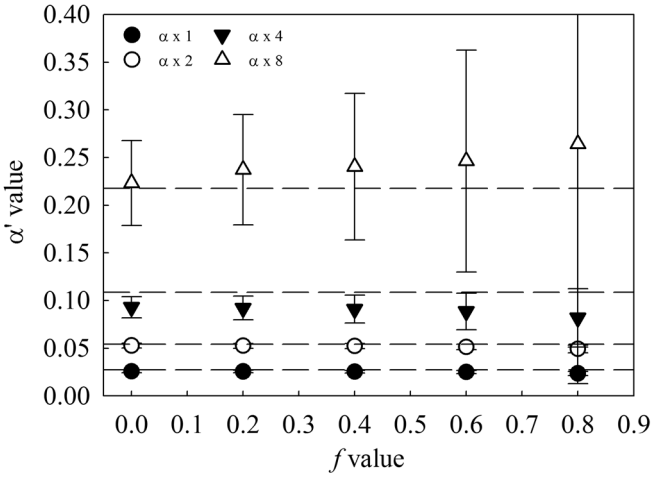

Fig. 7. Model calculations on α'estimates for a series of hypothetical ^{14}C time-course data with specified values of *f* and α (given by the dashed lines). A random error of up to 5% was introduced to simulate experimental noise to the test data set.

fitting algorithm does not provide accurate estimates of α at high contribution of HCO_3^- and high eCA activities (such as observed for *T. nitzschioides*). This occurs because the ^{14}C incorporation does not deviate strongly enough from a linear function. The errors in the model-derived α' estimates are smaller, however, when the HCO_3^- contribution is lower and moderate or no eCA activity is present. This approach, therefore, provides a means to estimate eCA activities with reasonable precision, provided that cells are not predominant HCO_3^- users ($f < 0.7$) and possess moderate amounts of eCA ($CA^{18O} < 4$). Unfortunately, high proportion of HCO_3^- uptake is often accompanied by high levels of eCA activities, especially when cells were acclimated under low CO_2 levels (e.g., Rost et al. 2003).

Assay conditions and limitations—Despite the close agreement in CO_2/HCO_3^- uptake ratios obtained by the different approaches, assay conditions differ in some aspects from the conditions under which cells are cultured, and this could potentially introduce some bias into the results. As disequilibrium techniques, both MIMS and ^{14}C approaches require the lack of eCA activity. In the present study this was achieved by treating cells with dextran-bound sulfonamide (DBS), a membrane-impermeable inhibitor of eCA (Sültemeyer et al. 1990). Since DBS prevents CA-mediated HCO_3^- use, the proportion of direct HCO_3^- or CO_2 uptake could also be altered by this treatment. Whereas the presence of DBS most likely will not affect the estimates on HCO_3^-/CO_2 uptake in species lacking eCA, the contribution of direct CO_2 uptake may be higher in situ when cells express extracellular CA activity. Inhibitors for eCA may also have other effects than eliminating eCA activity. It has recently been argued that CA inhibitors like acetazolamide (AZ) affect photosynthesis non-specifically over and above the effects on eCA activity (Pollock and Colman 2001, Martin and Tortell 2006). We therefore tested the effect of DBS on photosynthesis by comparing the ^{14}C fixation with our control. Whereas DBS and control samples always yielded similar rates of photosynthesis (compare final ^{14}C incorporation rates given in Fig. 2), the presence of the inhibitor AZ often resulted in lower incorporation rates (data not shown). Martin and Tortell (2006) suggested that AZ may affect the HCO_3^- transport system directly, leading to an underestimation of the HCO_3^- contribution to total C_i uptake and thus experiments with AZ-treated cells should be interpreted with caution.

The methods tested here are also limited to a certain pH range, i.e., rather low values of 8.0 for the MIMS and higher values of 8.5 for the ^{14}C approach. Since the pH strongly alters the speciation between CO_2 and HCO_3^- in the media, assay pH may directly influence the uptake ratio of the respective carbon species. The higher pH of the ^{14}C experiments, may favor HCO_3^- uptake by cells compared to that seen at pH 8.0. In addition, results also may be altered by pH effects unrelated to carbonate chemistry, such as by differences in the energy requirement to maintain internal pH (Raven & Lucas 1985). In view of the similar results obtained by the different methods, this influence can be considered small, at least for those species investigated in our study.

For both approaches, it is important that cells are not affected negatively over the entire course of the experimental assay. For instance, cells can be damaged during the process of harvesting or as a result of turbulent shear stress in the stirred cuvette. Oxygen accumulation over the duration of the assays (as a byproduct of photosynthesis in a closed system) also can alter photosynthesis and hence cause bias in the results. In the ^{14}C disequilibrium technique, a progressive decrease in photosynthetic net fixation would increase the difference between initial and final slope of the ^{14}C uptake curve, yielding a higher apparent CO_2 contribution to total carbon fixation. In the MIMS assay, a decrease in photosynthetic activity with time will cause underestimation of net fixation, CO_2 and HCO_3^- uptake and consequently lower apparent half-saturation constants of these processes. This effect would not, however, specifically affect the relative contributions of CO_2 and HCO_3^- uptake.

C_i flux measurements usually are performed across a range of C_i concentrations to yield the kinetics of CO_2 and HCO_3^- uptake. Hence, these experiments typically last longer than the ^{14}C disequilibrium assays, and consequently are more prone to introducing physiological stress on cells. It is therefore advisable to test the constancy of cellular activity by monitoring photosynthetic O_2 evolution over the assay time range in all species. None of the species investigated here showed a decline in photosynthesis under assay condition (data not shown). Elevated O_2 concentrations during MIMS assays can be counteracted by purging with N_2, prolonging the dark phases, or by working with lower cell densities.

Comments and recommendations—Our comparison of the MIMS and ^{14}C disequilibrium technique demonstrate that reliable and comparable estimations of the ratio of photosynthetic CO_2 and HCO_3^- uptake can be obtained. This was true for a variety of phytoplankton species from different taxonomic groups. The ^{14}C method can be regarded as a robust and accurate method, easily adaptable for field applications. For more detailed carbon flux studies, the MIMS technique offers a powerful tool as it also provides uptake kinetics and changes therein. This information is needed to fully characterize the CCM in phytoplankton and assess the CO_2 sensitivity of photosynthesis and C_i uptake.

Assessing extracellular CA activities by the ^{14}C approach allows accurate estimates of the acceleration in rate constants provided that cells are not predominant HCO_3^- users and possess moderate amounts of eCA. For estimates of eCA activities, covering a range of activities in CO_2 as well as HCO_3^- users, the MIMS provides a more accurate approach. It should be noted that values for absolute eCA activities cannot be compared directly between approaches.

In view of the general goal of adapting methods to low cell concentrations (resembling conditions of the natural environment) the carbon flux measurements by MIMS are limited by

the need to create a measurable chemical disequilibrium in the bulk solution. In this respect, the ^{14}C approach in which an isotopic disequilibrium is induced has a significant advantage for field studies, as it allows experiments to be conducted with cell densities closer to in situ values.

References

Aizawa, K., and S. Miyachi. 1986. Carbonic anhydrase and CO_2 concentrating mechanism in microalgae and cyanobacteria. FEMS Microbiol. Rev. 39:215–233.

Amoroso, G., D. Sültemeyer, C. Thyssen, and H. P. Fock. 1998. Uptake of HCO_3^- and CO_2 in cells and chloroplasts from the microalgae *Chlamydomonas reinhardtii* and *Dunaliella tertiolecta*. Plant Physiol. 116:193–201.

Badger, M. R., A. Kaplan, and J. A. Berry. 1977. The internal CO_2 pool of *Chlamydomonas reinhardtii*: Response to external CO_2. Carnegie Institute Year Book 76:362–366.

———, A. Kaplan, and J. A. Berry. 1980. Internal inorganic carbon pool of *Chlamydomonas reinhardtii*. Evidence for a CO_2 concentrating mechanism. Plant Physiol. 66:407–413.

———, K. Palmqvist, and J.-W. Yu. 1994. Measurement of CO_2 and HCO_3^- fluxes in cyanobacteria and microalgae during steady-state photosynthesis. Physiol. Plant. 90:529–536.

Berry, J. A., J. Boynton, A. Kaplan, and M. R. Badger. 1976. Growth and photosynthesis of *Chlamydomonas reinhardtii* as a function of CO_2 concentration. Carnegie Institute Wash Year Book 75:423–432.

Burkhardt, S., G. Amoroso, U. Riebesell, and D. Sültemeyer. 2001. CO_2 and HCO_3^- uptake in marine diatoms acclimated to different CO_2 concentrations. Limnol. Oceanogr. 46(6): 1378–1391.

Cassar, N., E. A. Laws, R. R. Bidigare, and B. N. Popp. 2004. Bicarbonate uptake by Southern Ocean phytoplankton, GlobalBiogeochem. Cycles 18, GB2003, [doi:10.1029/ 2003GB002116].

Chen, Y.-B., J. P. Zehr, and M. Mellon. 1996. Growth and nitrogen fixation of the diazotrophic filamentous non-heterocystous cyanobacterium *Trichodesmium* sp. IMS 101 in defined media: Evidence for a circadian rhythm, J. Phycol. 32(6):916–923.

Elzenga, J. T. M., H. B. A. Prins, and J. Stefels. 2000. The role of extracellular carbonic anhydrase activity in inorganic carbon utilization of *Phaeocystis globosa* (Prymnesiophyceae): A comparison with other marine algae using the isotope disequilibrium technique. Limnol. Oceanogr. 45(2): 372–380.

Espie, G. S., and B. Colman. 1986. Inorganic carbon uptake during photosynthesis. I. A theoretical analysis using the isotope disequilibrium technique. Plant Physiol. 80:863–869.

Giordano, M., J. Beardall, and J. A. Raven. 2005. CO_2 concentrating mechanisms in algae: mechanisms, environmental modulation, and evolution. Annu. Rev. Plant Biol. 56:99–131.

Graham, D., and C. P. Whittingham. 1968. The path of carbon during photosynthesis in *Chlorella pyrenoidosa* at high and low carbon dioxide concentrations. Z. Pflanzenphysiol. 58: 418–427.

Guillard, R. R. L., and J. H. Ryther. 1962. Studies of marine planktonic diatoms. Can. J. Microbiol. 8:229–239.

Johnson, K. S. 1982. Carbon dioxide hydration and dehydration kinetics in seawater. Limnol. Oceanogr. 27:849–855.

Kaplan, A., M. R. Badger, and J. A. Berry. 1980. Photosynthesis and the intracellular inorganic carbon pool in the bluegreen alga *Anabaena variabilis*: Response to external CO_2 concentration. Planta 149:219–226.

Laws, E. A., B. N. Popp, R. R. Bidigare, U. Riebesell, S. Burkhardt, and S. G. Wakeham. 2001. Controls of the molecular distribution and carbon isotopic composition of alkenones in certain haptophyte algae, Geochem. Geophys. Geosyst. 2000GC000057.

Martin, C. L., and P. D. Tortell. 2006. Bicarbonate transport and extracellular carbonate anhydrase in Bering Sea phytoplankton assemblages: Results from isotopic disequilibrium experiments. Limnol. Oceanogr. 51(5):2111–2121.

Nimer, N. A., M. Warren, and M. J. Merrett. 1998. The regulation of photosynthetic rate and activation of extracellular carbonic anhydrase under CO_2-limiting conditions in the marine diatom *Skeletonema costatum*. Plant Cell Environ. 21:805–812.

Palmqvist, K., J.-W. Yu, and M. R. Badger. 1994. Carbonic anhydrase activity and inorganic carbon fluxes in low- and high-C_i cells of *Chlamydomonas reinhardtii* and *Scenedesmus obliquus*. Physiol. Plant. 90:537–547.

Pollock, S. V., and B. Colman. 2001. The inhibition of the carbon concentrating mechanism of the green alga *Chlorella saccharophila* by acetazolamide. Physiol. Planta 111: 527–532.

Raven, J. A., and W. J. Lucas. 1985. Energy costs of carbon acquisition. p. 305-324. *In* W. J. Lucas and J. A. Berry [eds], Inorganic Carbon Uptake by Aquatic Photosynthetic Organisms, The American Society of Plant Physiologists, Rockville, MD, USA.

Reed, M. L., and D. Graham. 1981. Carbonic anhydrase in plants: Distribution, properties and possible physiological roles, p 47–94. *In* L. Reinhold, J. B. Harborne and T. Swain [eds], Progress in Phytochemistry, v. 7, Pergamon Press, Oxford.

Riebesell, U., D. A. Wolf-Gladrow, and V. Smetacek. 1993. Carbon dioxide limitation of marine phytoplankton growth rates. Nature 361:249–251.

Rost, B., U. Riebesell, S. Burkhardt, and D. Sültemeyer. 2003. Carbon acquisition of bloom-forming marine phytoplankton. Limnol. Oceanogr. 48(1):55–67.

———, K.-U. Richter, U. Riebesell, and P. J. Hansen. 2006. Inorganic carbon acquisition in red tide dinoflagellates, Plant Cell Environ. 29:810–822.

Silverman, D. N. 1982. Carbonic anhydrase. Oxygen-18 exchange catalyzed by an enzyme with rate-contributing proton-transfer steps. Methods Enzymol. 87:732–752.

Sültemeyer, D. F., H. P. Fock, and D. T. Canvin. 1990. Mass spectrometric measurement of intracellular carbonic anhy-

drase activity in high and low C_i cells of *Chlamydomonas*. Plant Physiol. 94:1250–1257.

Sültemeyer, D., C. Schmidt, and H. P. Fock. 1993. Carbonic anhydrases in higher plants and aquatic microorganisms. Physiol. Plant. 88:179–190.

———, G. D. Price, J.-W. Yu, and M. R. Badger. 1995. Characterization of carbon dioxide and bicarbonate transport during steady-state photosynthesis in the marine cyanobacterium *Synechococcus* strain PCC7002. Planta 197:597–607.

Tortell, P. D. 2000. Evolutionary and ecological perspectives on carbon acquisition in phytoplankton. Limnol. Oceanogr. 45(3):744–750.

——— 2005. Dissolved gas measurements in oceanic waters made by membrane inlet mass spectrometry. Limnol. Oceanogr.: Methods 3:24–37.

———, and F. M. M. Morel. 2002. Sources of inorganic carbon for phytoplankton in the eastern Subtropical and Equatorial Pacific Ocean. Limnol. Oceanogr. 47(4):1012–1022.

———, C. L. Martin, and M. E. Corkum. 2006. Inorganic carbon uptake and intracellular assimilation by Pacific phytoplankton assemblages. Limnol. Oceanogr. 51(5):2102-2110.

Submitted 4 December 2006
Revised 6 July 2007
Accepted 25 July 2007